THEORETICAL RESEARCH OF THE INTERNAL GAS DYNAMICS PROCESSES OF MEASUREMENTS OF HOT AIR CURTAIN WITH CROSS-FLOW FAN

MARIA R. KOROLEVA[1], OLGA V. MISHCHENKOVA[2], MICHAL KELEMEN[3], ALENA A. CHERNOVA[4]

[1]Udmurt Federal Research Center, Ural Branch, Russian Academy of Sciences, Izhevsk, Russian Federation

[2]Faculty of Mathematics and Natural Sciences Kalashnikov Izhevsk State Technical University, Izhevsk, Russian Federation

[3]Faculty of Mechanical Engineering, Technical University of Kosice, Institute of Automation, Mechatronics and Robotics,

Department of Mechatronics, Kosice, Slovak Republic

[4]Faculty of Mathematics and Natural Sciences and Faculty of Mechanical Engineering, Kalashnikov Izhevsk State Technical University, Izhevsk, Russian Federation

DOI: 10.17973/MMSJ.2020_06_2020028

e-mail: michal.kelemen@tuke.sk

This paper describes problems of computational simulation of gas dynamics and thermophysical processes running inside a displacement volume of the air curtain with a cross flow fan. The measurement of flow structure in the form of flow lines, gas pressure, temperature and velocity field at a fan rotation rate ranged from 250 rpm up to 1500 rpm is evaluated due to the computational experiment. The measurement shows that flow structure does not depend on the fan rotation rate and correspond to the experimental date. Velocity profiles are self-similar. Maximum vacuum pressure depending on the impeller rate is evaluated and local temperature maximums correspond the flow jet axis in the air curtain outlet cross section was estimated. Gas temperature in the vortex zone decreased up to 296 K and does not depend on the fan rotation rate that makes it possible to study the air curtain operation using the uncompressed liquid model. The linear relation between fan rotation rate and air capacity injected by a fan was demonstrated and described.

KEYWORDS

theoretical research, air curtain, cross-flow fan, computational simulation, gas dynamic, curtain efficiency.

1 INTRODUCTION

Maintenance of premises with high human or vehicle passing flow considers heat losses though opening spaces like unloading ports, doors and gates. Such premises are hospitals, schools, kinder gardens, sport and social objects, airports, railway stations and other service organizations (shops, theatres, hotels, restaurants), public transport, industrial and warehouse buildings. Temperature and air purity control in the building within specified limits can be performed by applying special electric-mechanical device – air curtain [Hyulla 2019]. In some cases, air curtains are used in order to provide special technological requirements such as food storage as air curtain can both cut down cold air during winter and supply hot air in summer. Besides, air curtains prevent the premise from penetration of insects, dust, smoke, bad odor etc. But mostly air curtains are applied for bordering the zones with various ambient temperature from different sides of the open doorway.

Air curtains differ in designation, heat source (including type of heating unit), type of mounting, air flow rate, displacement and geometry (body cross section, nozzle shape). One of the main elements of air curtain is a fan. As a rule, such devices include radial-flow or cross-flow fans.

Cross-flow or tangential fan is a device in which air mass moves perpendicularly to the axis of runner motion [Murcinkova 2013]. Body of the device is similar to the body of radial type one. Runner of the cross-flow fan is a cylinder with external surface formed by set of flow-shaped blades [Casarsa 2011] that ensure required blowdown in plane perpendicular to fan axis. Thus, the sucking surface is upper horizontal plane of the device (its length is the same as the length of the device) instead of side surface. The air mass is mixed with blades and the diffusor increases speed in a required direction [OpenFoam 2019].

Devices equipped with cross-flow (or tangential) fans have high values of gas dynamics parameters as well as high air consumption, low lift and low noise level [Casarsa 2011, OpenFoam 2019].

Advantages of cross-flow fans are:

- High efficiency;
- Ability to regulate the flow in a required direction;
- Generation of unique flat and uniform air flow.

Cross-flow fans have wide range of applications such as:

- heating (fireplaces, floor mounted convectors);
- air conditioning (ceiling heating and cooling systems, air humidifiers, air curtains);
- cooling systems for commercial and residential property (bottled drinks refrigerated display cases, cold counters);
- telecommunication systems (cooling of electronic components);
- health care (diagnostic devices, X-ray devices, incubators);
- office equipment (copying devices, printers);
- delicatessen (cold counters, commercial dishwashers).

According to experimental data the gas motion inside the air curtain equipped with such fan can be characterized with high turbulence rate [Casarsa 2011, Cernecky 2015, Darmawan 2015, Diametrically 2019, Diskin 2003]. Fan displacement and curtain body geometry has a significant influence on total operation of the unit. Experimental researches provide enormous amounts of data describing cross-flow fan operation but all of them are aimed at a single model of studied curtain and cannot be applied for modernization of existing devices or design of new ones. In this case methods of computation of gas dynamics widely used for aerodynamic flotation simulation in various technical devices are more preferable.

Computational simulation is used both for studying the unsteady aerodynamics and heat exchange in operating (internal) spaces of devices [Khosrowpanah 1988, Kim 2008, Darmawan 2015, Sun 2015, Bako 2016, Baranov 2017, Sharfarets 2018, Pivarčiová 2019] and for calculation of shape and airstream axis course indoors after it is blown out of the air curtain [Diskin 2003, Menter 2003, Kruglova 2006, Frank 2014, Grigoriev 2016, Li 2016, Gilyazetdinov 2018, Diametrically 2019, Simulation 2019].

Computational studies of gas dynamic processes in an air curtain displacement volume are essential for device performance parameters estimation (air efficiency, noise level, narrowness and average temperature of exhausting flow,

aerodynamics losses in air curtain flow channel) as well as for air curtain design optimization i.e. workspace geometry in order to achieve the required output stream parameters.
The present research analyses of viscous, compressible and heat-conducting gas flow in the air curtain displacement volume is based on computational gas dynamics methods. For computational modelling libraries of OpenFoam 2.0 [OpenFoam 2019] public intergrable platform for solution of medium mechanics problems and on opportunities of Salome 8.3.0 [Principle 2019] public intergrable platform are used [Krenicky 2011, Smeringaiova 2017, Rimar 2018, Ruzbarský 2020].

2 PROBLEM STATEMENT

The article provides the analysis of results obtained after numerical simulation of measurement of compressible viscous gas in an air curtain body displacement volume equipped with cross-flow fan (Fig. 1). Cross-flow fan consisting of impeller 1, inlet duct 2, output diffusor 3 and body 4 (Fig. 1b). Impeller includes 36 uniformly displaced flow shaped blades are considered.

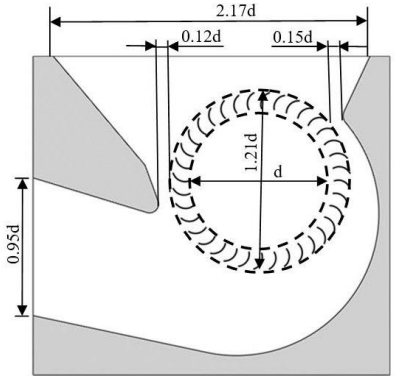

a)

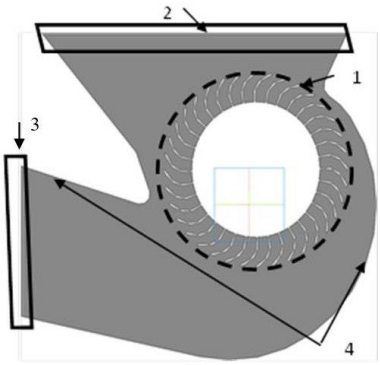

b)

Figure 1. Air curtain: a) cross section, b) computational area

The following assumptions and simplifications are used during simulation:
– the impeller rotates with a given constant speed and stationary operating condition of a fan is considered;
– gas (air) is characterized with constant viscosity and heat conduction factor;
– the problem is solved in two-dimensional formulation (Fig. 1b).
Research [Toffolo 2005] states that uniform profile of injected air independent of axial coordinate directed along fan impeller axis is generated in air curtain outlet. Obvious two-dimensional flow in the outlet cannot exist without two-dimensional flow in whole area and this allows us to study internal air curtain gas dynamics in two-dimensional formulation.

3 MATHEMATICAL SIMULATION

For mathematical simulation of air curtain internal volume air flow (Fig. 2) viscous compressed gas motion equation system is solved and includes additional condition equation:

$$\frac{\partial \rho}{\partial t}+\frac{\partial \rho u_i}{\partial x_i}=0 \tag{1}$$

$$\frac{\partial \rho u_i}{\partial t}+\frac{\partial \rho u_i u_j}{\partial x_j}=-\frac{\partial p}{\partial x_i}+$$

$$+\frac{\partial}{\partial x_j}\left(\mu\left(\frac{\partial u_i}{\partial x_j}+\frac{\partial u_j}{\partial x_i}\right)-\frac{2}{3}\mu\frac{\partial u_k}{\partial x_k}\delta_{ij}\right)+F_i \tag{2}$$

$$\frac{\partial \rho E}{\partial t}+\frac{\partial \rho E u_j}{\partial x_j}=-\frac{\partial p u_j}{\partial x_j}+\frac{\partial u_i \tau_{ij}}{\partial x_j}+$$

$$+\frac{\partial q_j}{\partial x_j}+F_i u_i \tag{3}$$

$$p=\rho RT \tag{4}$$

In given above formulas (1)-(4) following designations are specified:
ρ – density;
u_i – velocity components ;
p – pressure;
μ dynamic-viscosity coefficient;
Fi – external volume force;
$E=C_v T+0.5u_i^2$ – total specific energy;
$H=E+p/\rho=C_p T+0.5u_i^2=h+0.5u_i^2$ – total specific enthalpy;
$\tau_{ij}=2\mu S_{ij}-\frac{2}{3}\mu\frac{\partial u_k}{\partial x_k}\delta_{ij}$ – viscous stress tensor;
$S_{i,j}=\frac{1}{2}\left(\frac{\partial u_i}{\partial x_j}+\frac{\partial u_j}{\partial x_i}\right)$ – strain velocity tensor;
$q_j=\lambda\frac{\partial T}{\partial x_j}$ – heat flow;
λ – heat-conduction factor;
T – temperature;
R = 287 J/(kg·K) – specific gas constant.
The studied flow does not consider significant temperature falls thus coefficients of molecular viscosity heat conductivity are considered as constant μ = 1.85·10-5 Pa·s, λ = 0.0259 W/(m·K).
Initial equations are averaged according to Favre [20]. Values are given as a sum $\theta=\tilde{\theta}+\theta''$, where $\tilde{\theta}=\overline{\rho\theta}/\overline{\rho}$, where $\overline{\rho\theta}$, $\overline{\rho}$ - averaged parameters according to the Reynolds procedure. Thus, θ'' includes both turbulent and density fluctuation. Navier-Stocks averaged system is following:

$$\frac{\partial \bar{\rho}}{\partial t}+\frac{\partial \bar{\rho}\tilde{u}_i}{\partial x_i}=0 \quad (5)$$

$$\frac{\partial \bar{\rho}\tilde{u}_i}{\partial t}+\frac{\partial \bar{\rho}\tilde{u}_i\tilde{u}_j}{\partial x_j}=-\frac{\partial \bar{p}}{\partial x_i}+\frac{\partial}{\partial x_j}\left(\tilde{\tau}_{ij}+\tilde{\tau}_{tij}\right)+ + F_i \quad (6)$$

$$\frac{\partial \bar{\rho}\tilde{E}}{\partial t}+\frac{\partial \bar{\rho}\tilde{E}\tilde{u}_j}{\partial x_j}=-\frac{\partial \bar{p}\tilde{u}_j}{\partial x_j}+\frac{\partial}{\partial x_j}\left[\tilde{u}_i\left(\tilde{\tau}_{ij}+\tilde{\tau}_{tij}\right)\right]+ +\frac{\partial}{\partial x_j}\left(q_j+q_{tj}\right)+F_j\tilde{u}_j \quad (7)$$

$$\bar{p}=\bar{\rho}R\tilde{T} \quad (8)$$

In formulas (5)-(8) following designations are specified:

$\tilde{\tau}_{ij}=\mu\left(\frac{\partial \tilde{u}_i}{\partial x_j}+\frac{\partial \tilde{u}_j}{\partial x_i}\right)-\frac{2}{3}\mu\frac{\partial \tilde{u}_k}{\partial x_k}\delta_{ij}$ - Viscous stress tensor averaged according to Favre;

$\tilde{\tau}_{tij}=-\overline{\rho u_i'' u_u''}=\mu_t\left(\frac{\partial \tilde{u}_i}{\partial x_j}+\frac{\partial \tilde{u}_j}{\partial x_i}-\frac{2}{3}\frac{\partial \tilde{u}_k}{\partial x_k}\delta_{ij}\right)-\frac{2}{3}k\bar{\rho}\delta_{ij}$ - strain velocity tensor averaged according to Favre;

$\mu_t=\bar{\rho}\nu_t$ - turbulent viscosity dynamic coefficient;

$k=\frac{\overline{\rho u_i'' u_i''}}{2\bar{\rho}}$ - turbulent motion specific kinetic energy;

ω - specific turbulent dissipation;

$\varepsilon=C_\mu k\omega$ - turbulent dissipation;

$q_{tj}=-\overline{\rho u_i'' h''}$ - eddy heat flux.

Turbulent viscosity is calculated according to the SST [Chauhan 2006] turbulence model by following equations:

$$\frac{\partial \bar{\rho}k}{\partial t}+\frac{\partial \bar{\rho}k\tilde{u}_j}{\partial x_j}=\tilde{P}_k-\beta\bar{\rho}k\omega+ +\frac{\partial}{\partial x_j}\left[\left(\mu+\sigma_k\mu_t\right)\frac{\partial k}{\partial x_j}\right] \quad (9)$$

$$\frac{\partial \bar{\rho}\omega}{\partial t}+\frac{\partial \bar{\rho}\omega\tilde{u}_j}{\partial x_j}=2\alpha\bar{\rho}S_{ij}S_{ij}-\beta\bar{\rho}\omega^2+ +\frac{\partial}{\partial x_j}\left[\left(\mu+\sigma_k\mu_t\right)\frac{\partial k}{\partial x_j}\right]+ +2\left(1-F_1\right)\bar{\rho}\sigma_{w2}\frac{1}{\omega}\frac{\partial k}{\partial x_j}\frac{\partial \omega}{\partial x_j} \quad (10)$$

Where

$$P_k=\mu_t\frac{\partial u_i}{\partial x_j}\left(\frac{\partial u_i}{\partial x_j}+\frac{\partial u_j}{\partial x_i}\right)\rightarrow\tilde{P}_k=\min\left(P_k,10\beta\bar{\rho}k\omega\right)$$

Transition function is determined as

$$F_1=\tanh\left\langle\left\{\min\left[\max\left(\frac{\sqrt{k}}{\beta\omega y},\frac{500\nu}{y^2\omega}\right),\frac{4\bar{\rho}\sigma_{w2}k}{CD_{k\omega}y^2}\right]\right\}^4\right\rangle$$

Where $CD_{k\omega}=\max\left(2\bar{\rho}\sigma_{w2}\frac{1}{\omega}\frac{\partial k}{\partial x_j}\frac{\partial \omega}{\partial x_j},10^{-10}\right)$,

y - distance to the nearest wall. Value F_1 is zero far form solid interface ($k-\varepsilon$ model is used) and is changed to $k-\omega$ model inside the transition layer.

The turbulent viscosity coefficient itself is calculated by the following formula

$$\mu_t=\frac{\bar{\rho}a_1k}{\max\left(a_1\omega,\sqrt{2S_{ij}S_{ij}}F_2\right)} \quad (11)$$

Where second transition function F_2 is calculated as

$$F_2=\tanh\left\{\left[\max\left(\frac{2\sqrt{k}}{\beta\omega y},\frac{500\nu}{y^2\omega}\right)\right]^2\right\} \quad (12)$$

All constants of a model in equations (9), (10) are calculated according to the values from standard models $k-\varepsilon$ and $k-\omega$ as $\alpha=\alpha_1F+\alpha_2\left(1-F\right)$ etc.

Constants of the given model are: $\beta=0.09$, $\alpha_1=5/9$, $\alpha_2=0.44$, $\beta_1=3/40$, $\beta_2=0.0828$, $\sigma_{k1}=0.85$, $\sigma_{k2}=1$, $\sigma_{\omega1}=0.5$, $\sigma_{\omega2}=0.856$, $a_1=0.31$.

4 COMPUTATION GRID AND BOUNDARY CONDITIONS

In order to clearly describe the process of air suction and its exhaustion through outlet nozzle of the curtain a complex multiple block area was designed and it includes 4 zones (Fig. 2): 1 – inlet zone (air suction), 2 inner volume of the air curtain, 3 – fan, 4 – outlet zone (air exhaustion). Zones 1, 2 and 4 are motionless, zone 3 rotates with set angular velocity Ω. The grid in rotating and steady areas is flat and consists of triangle element. Total amount of elements is 18366 cells for all zones and 4677 cells for zone 3.

In this paper the problem was solved using approach [22] that takes local rotating reference frame in the impeller area (zone 3). This leads to transformation of basic Navier-Stocks equations in a rotation zone and, in order to take into account the rotation effect, initial equations (6) and (7) in this zone have additive component that consider the Coriolis force

$$F=\Omega\times u \quad (13)$$

This approach is used for simulation of the steady flows. Accordingly, body and grid around it in a rotation zone do not rotate physically. This approach, from computational point of view, is less demanding comparing to nonstationary simulation

and in case the problem was stated correctly it ensures close approximation and lower computational cost along with less calculation time.

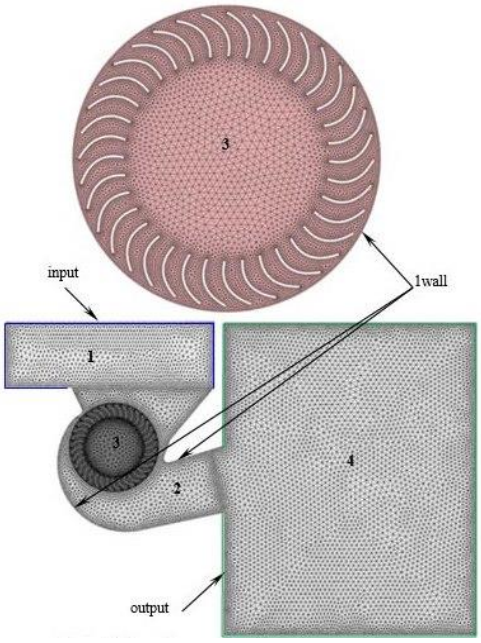

Figure 2. Finite volume grid and boundary conditions

Boundary conditions for (5) – (13) equation system are given in table 1.

	Parameter		Condition
Domain boundary	Rotating zone	Fan blades	$\frac{\partial p}{\partial n}=0,\ \frac{\partial T}{\partial n}=0,$ $u=0$
	Steady zone	Input	$p_{total}=10^5\,Па,$ $T=313K$
		Output	$p_{out}=10^5\,Па$
		Body wall	$\frac{\partial p}{\partial n}=0,\ \frac{\partial T}{\partial n}=0,$ $u=0$
	Rotation rate		250-1500 rpm

Table 1. Boundary conditions

5 CALCULATION RESULTS

As a result of air circulation computational simulation in air curtain internal volume, flow structure presented as flow line, pressure filed, gas temperature and speed in fan rotating with rate from 250 rpm to 1500 rpm was obtained. In addition to this, gas velocity and temperature profiles on the output boundary (outlet nozzle cutoff) were built up. Correlation of air curtain efficiency with rotation rate was determined on measurement of flow structure.

The measurement of flow lines and main parameters distribution field comparison showed that the flow structure doesn't depend on the fan blades rotation rate and is the same for all operation modes (Fig. 3).

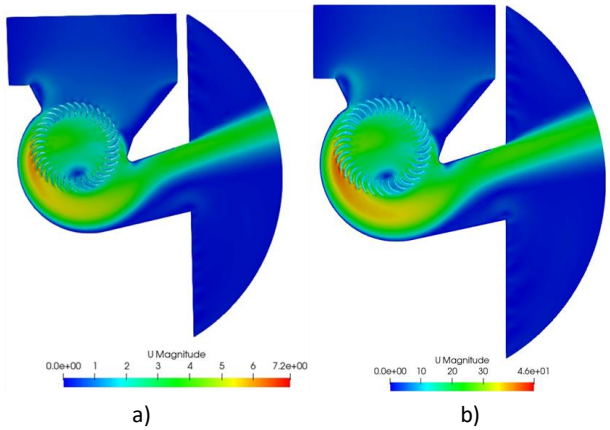

Figure 3. Velocity filed in air curtain cross-section for fan rotation rate: a) 250 rpm; б) 1500 rpm

Figure 4 shows velocity longitudinal component profiles on an outlet nozzle cutoff of air curtain at various rotation rates. It is obvious, that reverse flow zone displacement is the same for all rates and maximum velocity value (positive and negative) and increases along with rotation rate increase. The measurement shows that if the fan rotates at rate of 250 rpm maximum velocity is 3.62 m/s, if the fan rotates at rate of 1500 rpm maximum velocity is 24.56 m/s. Velocity profile analysis showed gas dimensionless velocity self-similarity (Fig. 4b).

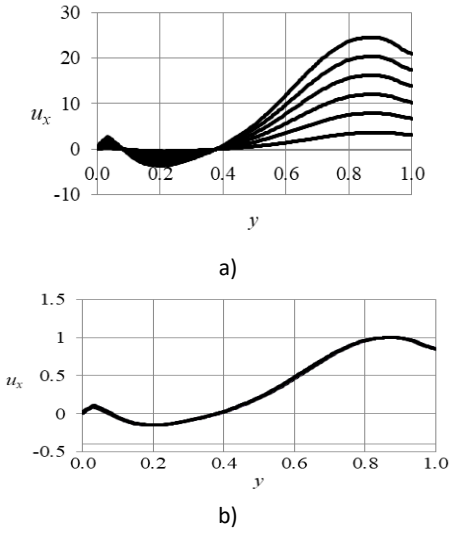

Figure 4. Longitudinal velocity component profile in the nozzle cross-section at different fan rotation rates: a) dimensional, b) dimensionless profiles

Let's consider gas flow peculiarities in the air curtain displacement volume (Fig, 3-6). Fan supplies air into curtain displacement volume and then air flow is directed to the impeller though inlet nozzle. A part of the flow moves though the back wall of the curtain and the other part gets inside the impeller and then comes out speeding up the gas.

After that, air flow is directed to the lower portion of the curtain and is exhausted into the atmosphere. However, some part of the main gas flow doesn't manage to go through the thin clearance between impeller blades and curtain front wall and returns inside the impeller thus creating reversal flow 3 (Fig. 5) that after contacting with incoming air is moved from fan axis down to the blades. Generated stationary vortex shedding zone 3 becomes a structural separator between suction and injection zones and corresponds to the experimental researches [23]. Interaction of the reverse flow with the main flow directed into the nozzle generates flow

separation line upstream the nozzle 5 (Fig. 5) and generates over-expanded jet pressed to the nozzle upper wall. Over-expanded jet generation in the nozzle exit is followed by the flow cut that generates the area with low pressure and reverse flow 4 (Fig. 5).
Results should be summarized briefly and main authors scientific contributions should be demonstrated.
Flow separation is followed by flow restructuring near the outlet nozzle upper wall and flow redirection. Asymmetric vortex pair 2 (Fig. 5) is generated in a cut point between inlet duct and air curtain front wall which is a result of interaction of vortex flow and an incoming air.

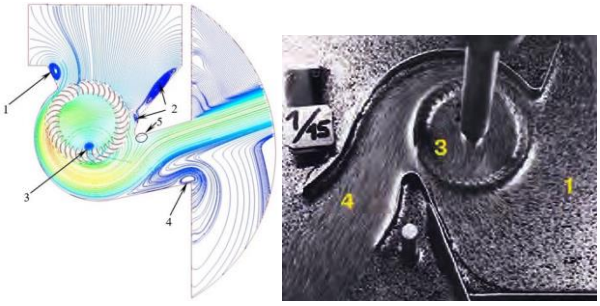

a) b)

Figure 5. Gas flow structure in air curtain: a) calculation; b) experiment [Toffolo 2005]

One more distinctive feature of the flow is fixed vortex generation 1 (Fig. 5) in the inlet cross- section near the back wall displaced due to the inlet cross-section geometry of air curtain and body design.
Given air flow pattern is common for all considered fan rotation rates. Exhaust jet parameters differ only with maximal speed value that varies from 4.6 m/s (250 rpm) to 25 m/s (1500rpm).
However, fan rotation rate does not influence the size, position and shape of the vortex zones.
Fig. 6 shows static pressure and temperature fields in the air curtain displacement volume. Local pressure and temperature distribution characteristics along the cross-section of the air curtain defined by the flow structure can be observed. Thus, local gas pressure and temperature minimum corresponds to the vortex area 3 position on Fig. 5. Pressure reduction against atmospheric pressure depends on impeller rotation rate and ranges from 20Pa at 250rpm to 1000Pa at 1500rpm.

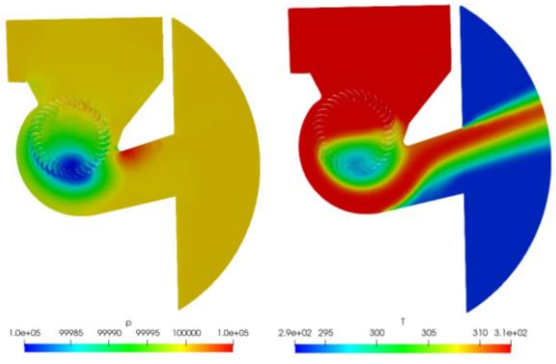

a) b)

Figure 6. Field: a) of static pressure; b) of temperature

Temperature field analysis showed the temperature field profile identity (Fig. 7) on the outlet nozzle cutoff at studied fan rotation rates.

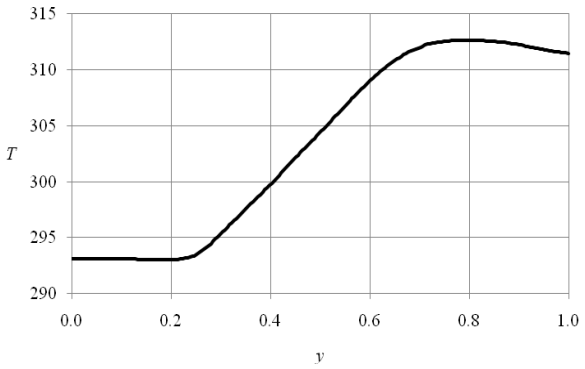

Figure 7. Temperature profile in the nozzle cross-section

Local temperature maximums correspond to the flow jet axis in the air curtain outlet cross section. Gas temperature in a vortex zone decreases to 296 K and does not depend on the fan rotation rate.
Curtain efficiency correlation to the rotation rate is shown on Fig. 8. Numerical simulation showed linear dependence between fan rotation rate and air capacity injected by fan.
This correlation is approximated by the linear equation:

$$Q = 0.83|\Omega| - 44.07,\ R^2 = 1 \qquad (14)$$

where Q - air capacity in cbm/h, $|\Omega|$ - angular rotation rate absolute of the fan in rpm, R^2 - R-squared value.

6 CONCLUSIONS

The work presents the study of the flow of viscous, compressible and heat-conducting gas in the air curtain displacement volume based on computation.

The problem was solved with the following assumptions:

- runner rotation rate is constant;

- fan operation mode is stationary;

- gas (air) has constant viscosity and heat exchange coefficient;

- two-dimensional formulation of the task.

Simulation was based on the Favre averaged Navier-Stokes equations for viscous compressed gas.

In order to properly describe the air suction process and its exhaustion through the curtain outlet nozzle, a complex multi-block area was designed. The grid in rotating and steady zones is unstructured and consists of triangle elements. Total amount of elements is 18366 cells.

Flow structure in the form of flow lines, gas pressure, temperature and velocity field at a fan rotation rate ranging from 250 rpm up to 1500 rpm is evaluated. Gas velocity and temperature profiles on the outlet boundary (outlet nozzle cutoff) were generated.

It is shown that flow structure does not depend on the fan rotation rate and is the same for all considered operation models; velocity profiles are self-similar.

Topological singularities of gas flow in air curtain displacement volume were studied. The measurement showed that flow structure is typical for cross-flow fans operation and follows the experimental data. Besides, it has some special features. Geometry of air curtain internal parts forms an oversized flow on the outlet nozzle cross section which results in reverse air

flow generation. In order to increase the air curtain efficiency, the outlet diffusor geometry shall be changed and an increase of gap width between outside edge of the fan vane and body critical cross section shall be considered.

It is shown that local pressure and temperature distributive characteristics in air curtain cross section are determined by flow structure. Thus, pressure decreases compared to the atmosphere that depends on impeller rate and ranges from 20 Pa at 250 rpm to 1000 Pa at 1500 rpm.

Temperature field analysis showed identity of flow temperature profile on the outlet nozzle cutoff at the studied fan rotation rates. Local temperature maximums correspond to the flow jet axis in the air curtain outlet cross section. Gas temperature in the vortex zone decreases to 296 K and does not depend on the fan rotation rate. Thus, it is possible to study the air curtain operation using the uncompressed liquid model.

Linear relation between fan rotation rate and air capacity injected by fan was demonstrated.

After all results are analyzed we can conclude the following:

1. Air curtain operation parameters can be estimated based on the incompressible model.

2. Flow pattern (structure and flow characteristics) study can be performed after computational calculation for one impeller rate value.

3. The obtained results permit us to make recommendations for device geometry improvement and the computational experiment method can be applied for the study and upgrade of other air curtain models.

ACKNOWLEDGMENTS

The research is performed with financial support from Kalashnikov ISTU in line with the scientific project №ЧАА/20-30-07.

REFERENCES

[Bako 2016] Bako, B., Bozek, P. Trends in simulation and planning of manufacturing companies. In: Procedia Engineering, International Conference on Manufacturing Engineering and Materials, ICMEM 2016, 6-10 June 2016, Nový Smokovec, Slovakia, 2016, Vol. 149, pp. 571-575.

[Baranov 2017] Baranov, M., Bozek, P. et al. Constructing and calculating of multistage sucker rod string according to reduced stress. Acta Montanistica Slovaca, 2017, Vol. 22, Issue 2, pp. 107-115.

[Casarsa 2011] Casarsa, L., Giannattasio, P. Experimental study of the three-dimensional flow field in cross-flow fans. Journal Experimental Thermal and Fluid Science, 2011, Vol. 35, No. 6, pp. 948-959.

[Cernecky 2015] Cernecky, J. et al. Ionization impact on the air cleaning efficiency in the interior. Measurement Science Review, 2015, Vol. 15, No. 4, pp. 156-166.

[Darmawan 2015] Darmawan, S. et al. Turbulent flow analysis in auxiliary cross-flow runner of a Proto X-3 Bioenergy micro gas turbine using RNG K-ε turbulence model. Journal of Engineering and Applied Sciences, 2015, Vol. 10, No. 16, pp. 7086-7091.

[Diametrically 2019] Diametrically opposite (tangential) fans. Retrieved December 19, 2019, Available at: https://www.airpromvent.ru/shop/Diametralnye_tangencialnye_ventilyatory.html.

[Diskin 2003] Diskin, M.E. On the calculation of air curtains. Journal Ventilation, Heating, Air Conditioning, Heat Supply and Building Thermal Physics (ABOK), 2003, Vol. 7, pp. 58-65.

[Frank 2014] Frank, D., Linden, P. The effectiveness of an air curtain in the doorway of a ventilated building. Journal of Fluid Mechanics, 2014, Vol. 756, pp. 130-164.

[Gilyazetdinov 2018] Gilyazetdinov, R.A., Verigina, D.A. Numerical modeling of air modes in rooms. In: Proc. Technical and mathematical Sciences. Student scientific forum: Electr. collection of articles on the Mat. III International. student. scient.-pract. conf., 2018, Vol. 3, No. 3, pp. 17-22. Retrieved March 22, 2019. Available at: https://nauchforum.ru/archive/SNF_tech/3%283%29.pdf.

[Grigoriev 2016] Grigoriev, A.Yu., Zhignovskaya, D.V. The review and the analysis aero - and thermodynamic processes in an aperture with an air and thermal veil. Scientific journal NRU ITMO. Series Refrigeration and Air Conditioning, 2016, 4, Vol. 4, pp. 6-15.

[Grigoryev 2015] Grigoryev, A.Yu. et al. Heated air curtain starting operating modes. Journal of International Academy of Refrigeration, 2015, Vol. 2, pp. 40-45.

[Hyulla 2019] Hyulla, I.Ya. Passage of air in cross-flow fans. Retrieved December. 19, 2019. Available at: www.scat-technology.ru/article/vozduhopotok-v-ventilyatore/.

[Khosrowpanah 1988] Khosrowpanah, S., Fiuzat, A. Experimental Study of Cross-Flow Turbine. Journal of Hydraulic Engineering, 1988, Vol. 114, No. 3, pp. 299–314.

[Kim 2008] Kim, T.A., et al. Performance of a cross-flow fan with various shapes of a rear guider and an exit duct. Journal of Mechanical Science and Technology, 2008, Vol. 22, pp. 1876-1882.

[Li 2016] Li, J. et al. Window purifying ventilator using a cross-flow fan: Simulation and optimization. Building Simulation, 2016, Vol. 9, pp. 481-488.

[Chauhan 2006] V. Chauhan, et al. Numerical Modeling of Doorway Flow Induced by an Air Curtain. Collection of Technical Papers - 9th AIAA/ASME Joint Thermophysics and Heat Transfer Conference Proceedings, 2016, pp. 246-252.

[Krenicky 2011] Krenicky, T. Implementation of Virtual Instrumentation for Machinery Monitoring. In: Scientific Papers: Operation and Diagnostics of Machines and Production Systems Operational States: Vol. 4, RAM-Verlag, Lüdenscheid, 2011, pp. 5-8. ISBN 978-3-942303-10-1.

[Kruglova 2006] Kruglova, E.S. Development of resource-saving air-heat curtains to maintain the normalized parameters of the microclimate in the industrial premises of the agro-industrial complex. Chelyabinsk, 2006. 21 p.

[Menter 2003] Menter, F.R. et al. Ten years of industrial experience with the SST turbulence model. In: Hanjalić, K. (ed.) Proc. 4th. Int. Symp. on Turbulence, Heat and Mass Transfer. Begell House, 2003, 8 p.

[Murcinkova 2013] Murcinkova, Z., Krenicky, T. Implementation of virtual instrumentation for multiparametric technical system monitoring. In: SGEM 2013: 13th Int. Multidisciplinary Sci. Geoconf. Vol. 1: 16-22 June, 2013, Albena, Bulgaria. Sofia: STEF92 Technology, 2013. pp. 139-144. ISBN 978-954-91818-9-0.

[Nasibullin 2015] Nasibullin, R.R. et al. Estimation of efficiency of thermal gas-air curtain on the basis of numerical modeling.

Herald of Kazan Technological University, 2015, Vol. 18, pp. 191-194.

[OpenFoam 2019] OpenFoam. Free CFD Software. Retrieved March 22, 2019 from link: http://openfoam.org/.

[Pivarčiová 2019] Pivarčiová, E. et al. Interferometric measurement of heat transfer above new generation foam concrete. Measurement Science Review, 2019, Vol. 19, No. 4, pp. 153-160.

[Principle 2019] Principle of operation of fans. Retrieved December. 19, 2019 from link: http://tehnika.expert/klimaticheskaya/ventilyator/princip-raboty-i-kak-ustroen.html#i-4.

[Rimar 2018] Rimar, M. et al. Study of gaseous flows in closed area with forced ventilation. MM Science Journal, 2018, Vol. March, pp. 2188-2191.

[Ruzbarský 2020] Ruzbarský, J. Origin and spreading of cracks due to thermal fatigue in case of metal molds. MM Science Journal, 2020, Vol. March, pp. 3716-3722.

[Salome 2019] Salome. Version 8.3.0. Retrieved March 22, 2019 from link: www.salome-platform.org/.

[Sharfarets 2018] Sharfarets, B.P., Dmitriev, S.P. Modeling of turbulent fluid motion based on the boussinesq hypothesis. Overview. Journal Nauchnoe Priborostroenie, 2018, Vol. 28, No. 3, pp. 101-108.

[Simulation 2019] Simulation of the thermal state of the room in different heating systems using the software complex ANSYS. Retrieved March 22, 2019 from link: http://www.cadfem-cis.ru/news/single/modelirovanie-te-5/.

[Smeringaiova 2017] Smeringaiova, A., Wittner, M. Optimalization of functional properties of radial fans. MM Science Journal, 2017, Vol. December, pp. 1967-1971.

[Sun 2015] Sun, K. et al. Experimental and numerical investigations on the eccentric vortex of the cross flow fan. International Journal of Refrigeration, 2015, Vol. 50, pp. 146-155.

[Toffolo 2005] Toffolo, A. On the theoretical link between design parameters and performance in cross-flow fans: a numerical and experimental study. Computers & Fluids, 2005, Vol. 34, pp. 49-66.

CONTACTS:

Maria R. Koroleva Ph.D., Associate Professor

Udmurt Federal Research Center, Ural Branch,

Russian Academy of Science,Baramzinoy str., 34, 426000, Izhevsk,

Russian Federation,

koroleva@udman.ru